



UvA-DARE (Digital Academic Repository)

Novel, Moon and Mars, partial gravity simulation paradigms and their effects on the balance between cell growth and cell proliferation during early plant development

Manzano, A.; Herranz, R.; den Toom, L.A.; te Slaa, S.; Borst, G.; Visser, M.; Medina, F.J.; van Loon, J.J.W.A.

DOI

[10.1038/s41526-018-0041-4](https://doi.org/10.1038/s41526-018-0041-4)

Publication date

2018

Document Version

Other version

Published in

NPJ Microgravity

License

CC BY

[Link to publication](#)

Citation for published version (APA):

Manzano, A., Herranz, R., den Toom, L. A., te Slaa, S., Borst, G., Visser, M., Medina, F. J., & van Loon, J. J. W. A. (2018). Novel, Moon and Mars, partial gravity simulation paradigms and their effects on the balance between cell growth and cell proliferation during early plant development. *NPJ Microgravity*, 4(1), [9]. <https://doi.org/10.1038/s41526-018-0041-4>

General rights

It is not permitted to download or to forward/distribute the text or part of it without the consent of the author(s) and/or copyright holder(s), other than for strictly personal, individual use, unless the work is under an open content license (like Creative Commons).

Disclaimer/Complaints regulations

If you believe that digital publication of certain material infringes any of your rights or (privacy) interests, please let the Library know, stating your reasons. In case of a legitimate complaint, the Library will make the material inaccessible and/or remove it from the website. Please Ask the Library: <https://uba.uva.nl/en/contact>, or a letter to: Library of the University of Amsterdam, Secretariat, Singel 425, 1012 WP Amsterdam, The Netherlands. You will be contacted as soon as possible.

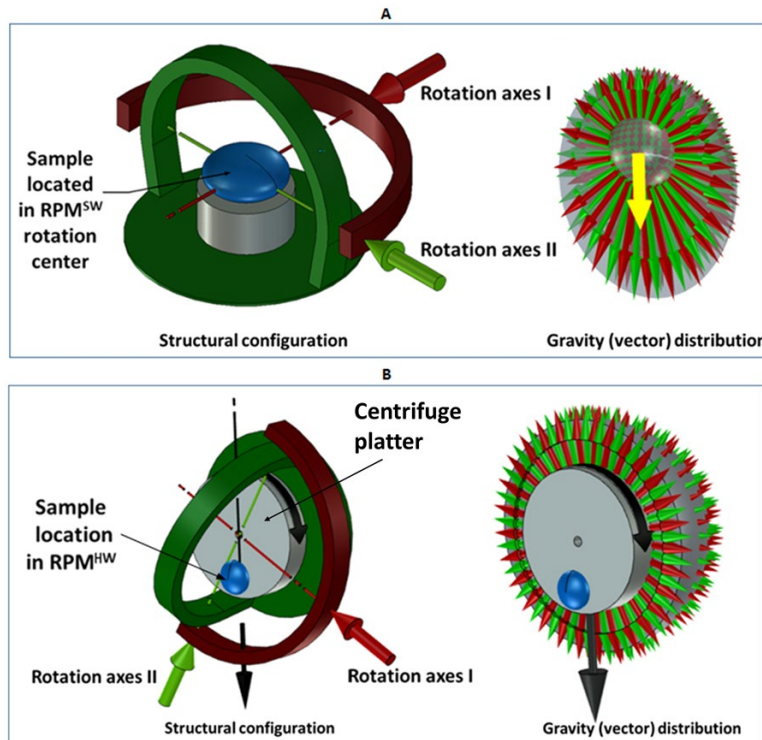
1 **Supplementary Information**

2

3 **Background of the Software RPM**

4 The RPM is a mechanism that consist of two perpendicular axed frames driven by motors that
5 continually rotate an experiment frame relative to the world frame (Figures 1 and S1). Or since
6 the gravity direction is fixed in the world frame, it continually rotates the gravity direction
7 relative to the experimental frame ergo the sample. The gravity vector acceleration can be
8 averaged over time resulting in a certain mean gravity ranging from the theoretical 0 g to 1 g
9 where 1 g is the Earth gravity acceleration of 9.81 m/s^2 . If the mean gravity is close to 0 g this is
10 called zero gravity or better microgravity, in order to take into account small deviations such as
11 distance from the center of rotation (see e.g. ^{1,2}). If the mean gravity is between 0 and 1 g it is
12 referred to as partial gravity or hypo-gravity. Note that the experiment must be placed in the
13 center of the experimental frames to prevent it from being exposed to possibly significant
14 centrifugal acceleration ^{1,3}.

15



16

17 *Figure S1: Set up of partial g simulation systems. A: Cartoon of the software directed simulated partial*
18 *gravity Random Positioning Machine (RPM^{SW}). Left the hardware / axes configuration. Right: Software*
19 *directing the motion of this RPM can be set to have a certain degree of preference along the Earth gravity*

20 vector. Resultant g represented by yellow arrow. B: The hardware directed simulated partial gravity
21 RPM (RPM^{HW}). Left the hardware configuration consisting of a regular (large size) RPM where the
22 partial g is generated by a centrifuge (grey). Right the resultant g -load depicted by the black arrow
23 pointing from the rotation axis of the centrifuge outwards.

24

25 Kinematics

26 The joint space of the mechanism is the set of motor angles (q_1, q_2) and forms a 2-plane. The
27 task space is the set of gravity directions relative to the experiment and forms a sphere (Figure
28 S2A). The sphere is embedded in 3-space and can be parametrized by the three components of
29 the gravity vector (g_1, g_2, g_3). The function from the motor angles to the gravity direction is
30 called the forward kinematics and is given by:

$$gravity(t) = forward(q) = \begin{bmatrix} \cos(q_1)\cos(q_2) \\ \cos(q_1)\sin(q_2) \\ \sin(q_1) \end{bmatrix}$$

31

32 where the motor angles can be identified with the latitude and longitude of a sphere. The inverse
33 function from the gravity direction to the motor angles is called the inverse kinematics.

34

35 The motor angles follow a defined path in joint space $q(t)$ that results in a certain gravity
36 direction path in task space $g(t)$. The goal is to set a motor path $q(t)$ such that the gravity path $g(t)$
37 has the desirable properties. In the following two such desirable properties for $g(t)$ will be
38 proposed and one algorithm for choosing a motor path $q(t)$ that has these properties. First they
39 will be discussed in the context of microgravity and later they will be generalized to partial
40 gravity.

41

42 Zero mean

43 The gravity vector $g(t)$ can be averaged over time resulting in a certain mean gravity:

44

$$mean(gravity(t)) = \frac{1}{t} \int gravity(t) dt$$

45

46 The first and most obvious desirable property is that the mean converges to zero or $(0, 0, 0)$.
47 Most algorithms from literature have this property^{4,5}. For example also a simple clinostat has it.
48 However, for some samples this may not be sufficient. Note that the rate of convergence must be
49 fast compared to the relevant time constants of the experiment. For example the perception time

50 for plants is in the order of seconds ⁶, for the single cell organism *Euglena gracilis*, a similar time
51 order of around five seconds has been reported ⁷.

52
53 **Uniform distribution**

54 The space of all gravity directions provides a sphere. The gravity path $g(t)$ walks over this sphere
55 and visits different points. The relative times that it spends in the neighborhoods of different
56 points result in a certain distribution over the sphere. If the path visits all points equally the path
57 converges to a uniform distribution (Figure S2A), and if it visits some points more than others
58 the path converges to a non-uniform distribution. A simple 2D clinostat for example only visits 1
59 great circle on the sphere (which can be identified with the equator of the sphere), and therefore
60 results in a very non-uniform distribution. Different distributions can result in same mean
61 gravity. For example both the uniform distribution and the clinostat distribution result in the
62 same zero mean.

63 Certain experiments may be more sensitive to gravity in some directions than in other directions,
64 and are therefore sensitive to the distribution of the gravity vector. Such experiments would
65 result in different outcomes for different distributions. Note that such experiments are also
66 sensitive to how the experiment is fixed in the experiment frame because the distribution is
67 relative to the experiment frame.

68 The only distribution that has no bias in certain directions is the uniform distribution. Therefore
69 the second desirable property of a gravity path is that the distribution converges to a uniform
70 distribution. Note that also here the rate of convergence must preferably be less compared to the
71 relative time constants of the experiment.

72 A good measure for the uniformity is the standard deviation of the density of the distribution
73 over surface of the sphere. Here density (t, q) is the amount of time the gravity direction has
74 spent in a neighborhood of $f(q)$.

$$\text{standard deviation}(\text{density}(q, t)) = \sqrt{\frac{1}{4\pi t} \iint \left(\text{density}(q, t) - \frac{t}{4\pi} \right)^2 \cos(q_1) dq_1 dq_2}$$

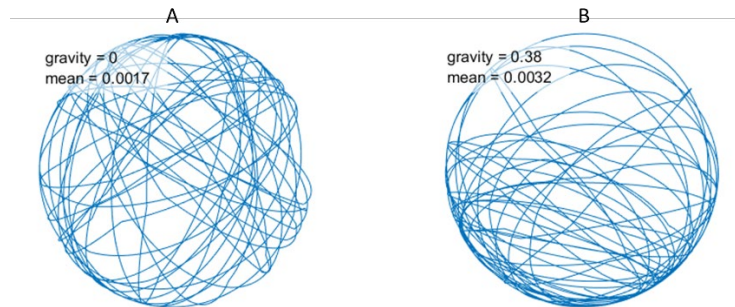
75
76 Most algorithms from literature (for example figure 4 of Wuest *et al.*⁴) including the algorithm
77 for the first generation of the RPM ² result in a uniform distribution in the latitude – longitude
78 plane. However, when this plane is folded around the sphere the density at the poles becomes
79 much higher than at the equator. This is similar to a globe where the density of meridians at the

80 poles is higher than at the equator. Although the first property (zero mean) is met, the second
81 property (uniform distribution) is not met.

82
83 **Random walk**

84 The gravity path that is proposed consists of a random walk over the surface of the sphere. The
85 random walk consists of a sequence of steps and turns. The steps are geodesic curves of a certain
86 length which on the surface of a sphere correspond to pieces of great circles. The turns are
87 uniformly distributed between plus or minus a defined maximum angle. It can be proven that
88 such a random walk converges to a uniform distribution over the sphere ⁸.

89



90

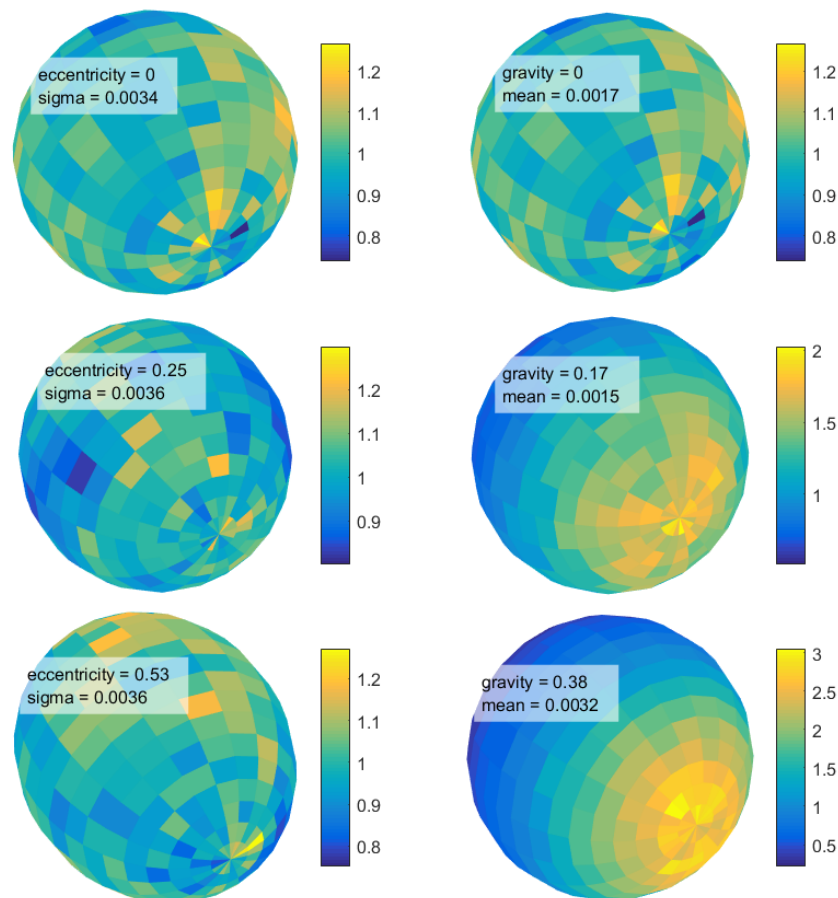
91 *Figure S2: The beginning of a path of the gravity vector over the sphere for zero gravity (on the left) and*
92 *for Mars (on the right). It can be seen that on the left the trajectory is distributed uniformly over the*
93 *sphere, while on the right it trajectory spends more time at the bottom than at the top, resulting in a*
94 *partial gravity factor of 0.38. Mean in the figure is the mean error between the desired and the actual*
95 *partial gravity factor after running for 1 hour.*

96

97 **Generalization to partial gravity**

98 The algorithm for zero gravity (random walk over a sphere) can be generalized to partial gravity
99 by introducing a prolate spheroid. A prolate spheroid is an ellipse that is rotated around its major
100 axis and has the shape of a rugby ball (see Figures 1B and S3). It has two focal points. One of the
101 focal points is fixed in the center of the sphere of gravity directions, and the other focal point is
102 moved in the direction of the desired partial gravity. Now instead of performing a random walk
103 over the sphere a geodesic random walk over the spheroid is performed. The resulting random
104 walk will converge to a uniform distribution over the spheroid. The proof from ⁸ still holds and
105 this random walk is then projected from the spheroid onto the sphere.

106 Because a relatively large part of the surface of the spheroid is on one side of the sphere and a
 107 relatively small part on the other side (Figure S2B), the gravity direction spends more time on
 108 that side of the sphere. So if the gravity vector is averaged over time, it converges to a certain
 109 non-zero partial gravity. By varying the ellipticity of the spheroid from 0 to 1 the simulated
 110 partial gravity is varied from 0 to 1.
 111 The two desirable properties can be generalized to partial gravity as follows. For the first
 112 property (zero mean) instead of looking at the norm of the mean gravity we look at the norm of
 113 the difference between the mean gravity and the desired partial gravity. For the second property
 114 (uniform density), instead of looking at the standard deviation of the density of the distribution
 115 over the sphere, we look at the distribution over the spheroid.
 116



117 *Figure S3: Distribution of the path over a spheroid (on the left) and resulting distribution of the gravity*
 118 *vector over the sphere (on the right) after running for 1 hour. The top row is for zero gravity (eccentricity*
 119 *of 0), the middle row for the Moon (eccentricity of 0.25 resulting in partial gravity of 0.17) and the*
 120 *bottom row for Mars (eccentricity of 0.53 resulting in a partial gravity of 0.38). The scale bars represent*
 121

122 *the normalized density where I is uniform density. One wants the pictures on the left to be as uniform as*
123 *possible. For the pictures on the right it depends on the desired partial gravity factor. Mean is the mean*
124 *error between the desired and the actual partial gravity factor. Sigma is the standard deviation of the*
125 *normalized density of the distribution relative to a uniform distribution.*

126

127 **References**

- 128 1 van Loon, J. J. W. A. (2007). Some history and use of the Random Positioning Machine, RPM, in gravity
129 related research. *Adv Space Res* 39, 1161-5.
- 130 2 Borst, A. G., van Loon, J. J. W. A. (2009). Technology and developments for the random positioning
131 machine, RPM. *Microgravity Sci. Technol* 21, 6.
- 132 3 Hasenstein, K. H., and van Loon, J. J. W. A. (2015). Clinostats and other rotating systems — Design,
133 function, and limitations. in “Generation and Applications of Extra-Terrestrial Environments on
134 Earth”, D.A. Beysens & J.J.W. A. van Loon (eds.). *River Publishers, Denmark*.
- 135 4 Wuest S.L., Richard S., Walther I., R Furrer R., Anderegg R., Sekler J., Egli M. (2014) A novel
136 microgravity simulator applicable for three dimensional cell culturing. *Microgravity Science and*
137 *Technology*, 26(2), 77 – 88.
- 138 5 Kim Y.J., Jeong A.J., Kim M., Lee C., Ye S.K., Kim S. (2017) Time-averaged simulated microgravity
139 (taSMG) inhibits proliferation of lymphoma cells, L-540 and HDLM-2, using a 3D clinostat. *Biomed*
140 *Eng Online*. 16:48, 1-12.
- 141 6 Perbal G., Jeune B., Lefranc A., Carnero-Diaz E., Driss-Ecole D. (2002) The dose–response curve of the
142 gravitropic reaction: a re-analysis. *Physiol Plant*. 114(3), 336-342.
- 143 7 Lebert M., Porst M., Richter P, Hader D.P. (1999) Physical characterization of gravitaxis in *Euglena*
144 *gracilis*. *J Plant Physiol*. 155(3), 338-343.
- 145 8 Jørgensen E. (1975) The central limit problem for geodesic random walks. *Zeitschrift für*
146 *Warscheinlichkeitstheorie und Verwandte Gebiete*. 32(1), 1 – 64.